

# Simultaneous estimation of wind shears and misalignments from rotor loads: formulation for IPC-controlled wind turbines

M. Bertelè<sup>1</sup>, C.L. Bottasso<sup>1,2</sup>, and S. Cacciola<sup>2</sup>

<sup>1</sup> Wind Energy Institute, Technische Universität München, Garching bei München, Germany

<sup>2</sup> Dipartimento di Scienze e Tecnologie Aerospaziali, Politecnico di Milano, Milano, Italy

E-mail: {marta.bertele, carlo.bottasso}@tum.de, stefano.cacciola@polimi.it

**Abstract.** In this paper, the turbine itself is used as an anemometer to estimate the inflow at its rotor disk. Indeed, given that any anisotropy in the wind will lead to periodic loads, by studying the machine response one can infer rotor-effective wind conditions and exploit such information for turbine and farm-level control applications. Specifically, expanding the idea of previous publications, the case of an individually pitch-controlled machine is considered herein: a linear implicit model is formulated to relate some characteristics of the wind—in the form of shears and misalignment angles—to the 1P harmonics of pitch angles and blade loads. The performance of the proposed algorithm is tested in a simulation environment, including both uniform and turbulent wind conditions.

## 1. Introduction

To improve the performance of a single wind turbine as well as of a wind farm, reliable information about the wind inflow can be of significant help. For example, accurate information about yaw misalignment can be used by a yaw control system to realign the turbine to the wind. When this information is of better quality than the one provided by the nacelle wind vane, this approach might lead to higher harvested power and lower fatigue loads. Similarly, the presence of a horizontal shear can be used for wake impingement detection, which can be used for the cooperative control of wind turbines within a wind power plant. Furthermore, measurements of the vertical shear can be used to better tune individual pitch control strategies (IPC) or to account for atmospheric stability, which has a strong effect on wake behavior and consequently on wind farm control strategies.

Unfortunately, accurate wind inflow measurements are still difficult to obtain. Commonly used devices such as met-masts measure an inflow that is not co-located with the turbine, and therefore is of only limited use. Wind vanes and anemometers, on the other hand, measure the wind at the nacelle, but this information is point-wise (as opposed to rotor-equivalent), and also affected by blade passage and nacelle interference effects. More accurate measurements can be obtained by LiDARs, which are however still not widely adopted and remain at the moment confined primarily to research applications. In general, it can be safely stated that wind turbines today are still largely unaware of the wind conditions in which they operate.

To overcome such hurdles, the idea of using the turbine as an anemometer was introduced in Ref. [1]. Following this approach, first in Ref. [2, 3] and then in [4, 5], the response of the



machine was used to infer rotor-effective wind conditions. Specifically, since any anisotropy in the wind leads to periodic loads [6], by measuring the 1P harmonic components of the blade out-of-plane and in-plane root bending moment, one can infer the wind field, as described by four parameters: vertical and horizontal misalignment angles (upflow and yaw angle, respectively), and vertical and horizontal shears.

In this paper, the formulation proposed in Ref. [4, 5] is extended and adapted to IPC-controlled machines. Given that such control systems aim at decreasing the loading on the machine by individually pitching each blade, in this work both blade loads and pitch harmonics are used to estimate the inflow. Since the only required hardware consists of blade load and pitch sensors, the proposed wind inflow estimator amounts to a software upgrade when such sensors are already available (for example, for load alleviating closed-loop control).

## 2. Formulation

### 2.1. Wind field parameterization

Exposed to a non-isotropic wind field, i.e. an inflow constant in time but not in space, the loading experienced by a rotating blade will be periodic, since periodic are the changes in relative velocity and therefore in angle of attack experienced by its airfoils. To describe such anisotropy, four parameters are defined as shown in Fig. 1: the yaw misalignment  $\phi$ , the vertical shear  $\kappa_v$ , the upflow angle  $\chi$ , and the horizontal shear  $\kappa_h$ , grouped together in the wind state vector:

$$\boldsymbol{\theta} = \{\phi, \kappa_v, \chi, \kappa_h\}^T. \quad (1)$$

The wind field is described as

$$V(y, z) = V_h \left( \left( \frac{z}{z_h} \right)^{\kappa_v} + \frac{y}{R} \kappa_h \right), \quad (2)$$

where  $V_h$  and  $z_h$  are the wind speed and the vertical coordinate at hub height, respectively, while  $R$  is the rotor radius. The three wind speed components can then be expressed as

$$u(y, z) = V(y, z) \cos \phi \cos \chi, \quad (3a)$$

$$v(y, z) = V(y, z) \sin \phi \cos \chi, \quad (3b)$$

$$w(y, z) = V(y, z) \sin \chi. \quad (3c)$$

### 2.2. Blade load and pitch harmonics

Under a steady anisotropic wind, the response of a stable wind turbine will converge to a periodic motion [6]. Therefore a generic load  $m$  of the  $i$ th blade can be expanded in Fourier series as

$$m_{(i)} = m_0 + m_{1c} \cos \psi_{(i)} + m_{1s} \sin \psi_{(i)} + \dots, \quad (4)$$

with  $\psi$  the azimuth angle,  $m_0$  the constant amplitude, subscripts 1c and 1s referring to the 1P cosine and sine component, respectively. Once three measured blade loads are available, sine and cosine  $n$ P harmonics can be readily computed using the Coleman transformation [7] as follows:

$$\begin{Bmatrix} m_{nc} \\ m_{ns} \end{Bmatrix} = \frac{2}{3} \begin{bmatrix} \cos(n\psi_{(1)}) & \cos(n\psi_{(2)}) & \cos(n\psi_{(3)}) \\ \sin(n\psi_{(1)}) & \sin(n\psi_{(2)}) & \sin(n\psi_{(3)}) \end{bmatrix} \begin{Bmatrix} m_{(1)} \\ m_{(2)} \\ m_{(3)} \end{Bmatrix}. \quad (5)$$

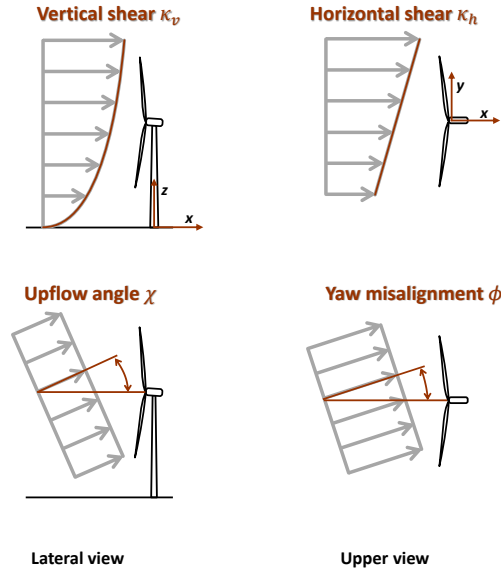


**Figure 1.** Parameterization of the wind inflow.

A similar approach can be used to extract the components of the blade pitch angle  $\beta$ . The 1P cosine and sine harmonics of both out- (OP) and in-plane (IP) loads and pitch are respectively grouped in vectors

$$\mathbf{m} = \{m_{1c}^{\text{OP}}, m_{1s}^{\text{OP}}, m_{1c}^{\text{IP}}, m_{1s}^{\text{IP}}\}^T \quad (6)$$

and

$$\boldsymbol{\beta} = \{\beta_{1c}, \beta_{1s}\}^T. \quad (7)$$

### 2.3. Wind state estimator

In this paper the idea of inferring the rotor effective inflow from the machine response is applied to the case of an IPC-controlled machine. When an IPC controller is used for load reduction, a different pitch demand is computed for each blade, exploiting the fact that each blade has its own independent pitch actuator. The blade pitch frequency is limited by the maximum pitch speed, and it is typically further limited to the 1P harmonic, since this allows for a reduction of the 1P blade loads and, in turn, of the 0P (constant) loads in the fixed frame. In the present work, the controller is implemented by combining a collective pitch and torque LQR formulation [8, 9] together with the proportional integral (PI) 1P IPC controller of Refs. [10, 11].

The linear model relating the response of the IPC-controlled machine to the wind parameters is formulated as follows

$$\mathbf{m} = \mathbf{F}(V)\boldsymbol{\theta} + \mathbf{G}(V)\boldsymbol{\beta} + \mathbf{m}_0(V), \quad (8)$$

where  $\mathbf{F}(V)$ ,  $\mathbf{G}(V)$  and  $\mathbf{m}_0(V)$  are the model coefficients scheduled with respect to the wind speed  $V$ . The effect of wind parameters on blade loads, i.e. the derivative of the latter with respect to the former, is represented by the coefficients grouped in matrix  $\mathbf{F}(V)$ , while the effect of the controller cyclic pitching is represented by matrix  $\mathbf{G}$ . Finally, vector  $\mathbf{m}_0(V)$  accounts for loading induced by gravity [5]. This formulation represents an extension of the one proposed in Refs. [4, 5], which now includes also the effects of pitch harmonics.

To identify the model coefficients given a specific wind speed, a rich enough set of measured  $\mathbf{m}_j$  and  $\boldsymbol{\beta}_j$  at the respective known  $\boldsymbol{\theta}_j$  has to be available. Grouping the  $j = 1, \dots, N$

experiments together, i.e.  $\mathbf{M} = [\mathbf{m}_1, \dots, \mathbf{m}_N]$ ,  $\mathbf{B} = [\beta_1, \dots, \beta_N]$  and  $\Theta = [\theta_1, \dots, \theta_N]$ , focusing here for brevity on one single wind speed  $\bar{V}$ , the system can be rewritten as

$$\mathbf{M} = \mathbf{F}(\bar{V})\Theta + \mathbf{m}_0(\bar{V}) + \mathbf{G}(\bar{V})\mathbf{B} = \mathbf{T}(\bar{V})\bar{\Theta}, \quad (9)$$

where  $\mathbf{T} = [\mathbf{F}(\bar{V}) \ \mathbf{G}(\bar{V}) \ \mathbf{m}_0(\bar{V})]$  and  $\bar{\Theta} = [\Theta \ \mathbf{B} \ \mathbf{1}]^T$ ,  $\mathbf{1}$  being the unit vector. Finally, the model coefficients grouped in  $\mathbf{T}$  can be identified in a least-square sense as

$$\mathbf{T}(\bar{V}) = \mathbf{M}\bar{\Theta}^T [\bar{\Theta}\bar{\Theta}^T]^{-1}. \quad (10)$$

Once the coefficients are known, one can exploit the model to infer the wind state parameters from the machine response. Indeed, given the measured  $\mathbf{m}_M$  and  $\beta_M$ , the estimated wind states  $\theta_E$  can be computed in a least-square sense as

$$\theta_E = (\mathbf{F}(V)^T \mathbf{F}(V))^{-1} \mathbf{F}(V)^T (\mathbf{m}_M - \mathbf{m}_0(V) - \mathbf{G}(V)\beta_M). \quad (11)$$

### 3. Results

#### 3.1. Simulation environment

To characterize the performance of the proposed formulation, the flexible multibody aeroservoelastic model of a 3 MW three-bladed horizontal-axis wind turbine was simulated. The machine hub height and rotor diameter are 80 and 93 m, respectively, while the cut-in, rated and cut-off wind speeds are 3, 12.5 and 25  $\text{ms}^{-1}$ , respectively, which include a wide region II $^{1/2}$  from 9 to 12.5  $\text{ms}^{-1}$ . The aeroelastic behaviour of the machine was simulated with the code Cp-Lambda [12], modeling blades and tower as geometrically exact non-linear beams, including a torsionally elastic drive-train and rotor-speed-dependent mechanical losses. The aerodynamics is rendered with the classical Blade Element Momentum theory, including hub and tip losses, unsteady corrections and dynamic stall.

Wind time histories were generated with the code TurbSim [13], for both turbulent and non-turbulent conditions. In the turbulent case, the wind histories were generated at a rotor-attached grid by adding turbulent fluctuations according to the Kaimal model to a steady flow characterized by given values of the four wind states. At each time instant, reference  $\theta$  values were then extracted by fitting Eq. (1) to the wind grid. Such reference values are considered as the *ground truth*, and they are subsequently used as terms of comparisons for the corresponding quantities computed by the estimator.

Several 3-minute long steady simulations were run with the IPC controller on and off, considering the combinations of the following parameter values:

$$V = \{11, 12, 15, 16, 17, 19\} \text{ ms}^{-1}, \quad (12a)$$

$$\phi = \{-16, -12, -8, -4, 0, 4, 8, 12, 16\} \text{ deg}, \quad (12b)$$

$$\kappa_v = \{0.0, 0.1, 0.2, 0.3, 0.4\}, \quad (12c)$$

$$\chi = \{0, 4, 8, 12\} \text{ deg}, \quad (12d)$$

$$\kappa_h = \{-0.1, -0.05, 0.0, 0.05, 0.1\}. \quad (12e)$$

The results of the simulations were then used to identify the model as described in §2.3. After having identified the model coefficients, the same set of simulations was then used to observe the wind conditions given measured blade loads and pitch angles.

Figure 2 shows the accuracy of the wind estimation in steady conditions for tests performed at 15  $\text{ms}^{-1}$  with the IPC controller turned on. Each subplot represents a different wind state. The reference wind parameter, i.e. the ground truth, is reported on the  $x$ -axis, while the observed one on the  $y$ -axis: ideally, results should fall exactly on the bisector line. Analyzing the results,

one can notice that the model is capable of correctly observing both shears, with a slight decrease in accuracy in the vertical shear observation when high positive yaw angles are considered. The upflow angle can as well be estimated with only slight inaccuracies, which nevertheless do not exceed  $2^\circ$ . Finally, the estimation of the wind direction appears to be very precise for angles that do not exceed  $\pm 12^\circ$ , after which a deviation of about  $3^\circ$  from the reference can be observed. A similar overall behaviour was noted at different wind speeds from the one considered here. Such inaccuracies, specifically the one concerning the yaw angle, are due to non-linearities in the load-wind relationship, which cannot be captured by the present linear formulation. This problem can be easily addressed by the use of a model with a prescribed level of non-linearity, which still results in a linear model-estimation problem [5].

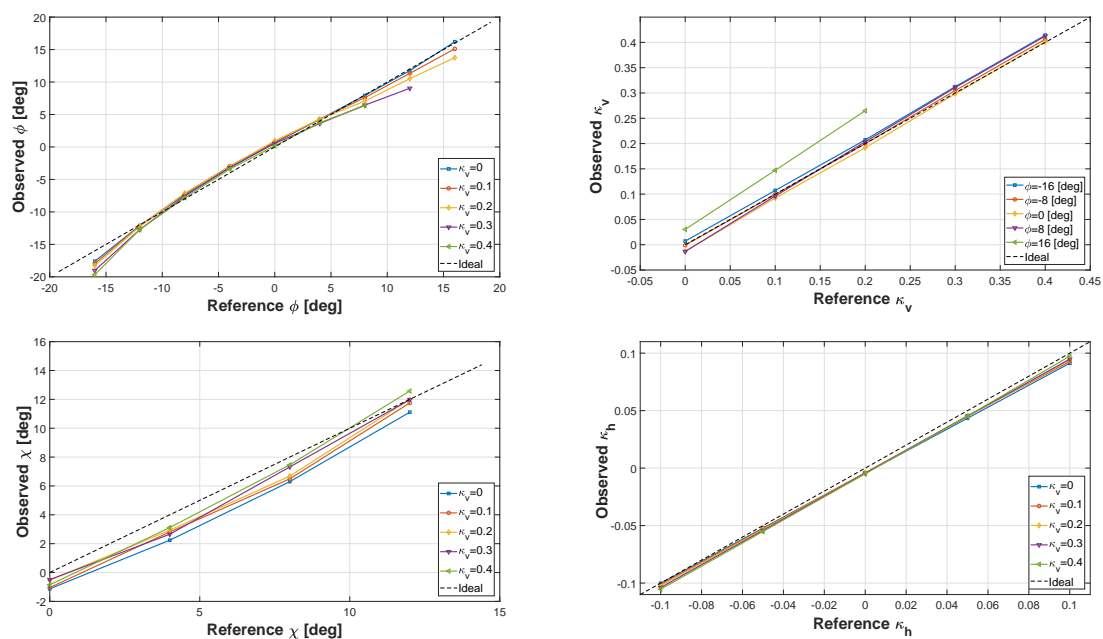


**Figure 2.** Wind states observed using the linear model for different steady inflow conditions at  $15 \text{ ms}^{-1}$ : yaw misalignment  $\phi$  at  $\chi = 8$  deg and  $\kappa_h = -0.1$  (top left), vertical shear  $\kappa_v$  at  $\chi = 8$  deg and  $\kappa_h = -0.1$  (top right), upflow angle  $\chi$  at  $\phi = -8$  deg and  $\kappa_h = -0.1$  (bottom left), horizontal shear  $\kappa_h$  at  $\chi = 8$  deg and  $\phi = -8$  deg (bottom right).

### 3.2. Non-turbulent wind conditions

To test the ability of the wind estimator in detecting changes in the wind parameters, different simulations were performed in non-turbulent wind conditions with the IPC controller turned on. In each simulation the wind speed was kept constant, whereas the wind parameters were varied independently from one another.

Figure 3 shows an excerpt of the results at  $17 \text{ ms}^{-1}$ . Wind parameters appear to be correctly estimated, with a very good accuracy as far as shears are concerned, and with only relatively small errors, not exceeding  $3^\circ$ , in the case of the angles. Similar results were obtained for different wind speeds, with an increase in accuracy at higher wind speeds. To ease the comparison, delays in the observed states induced by the 1P harmonic extraction procedure were eliminated from the figure.

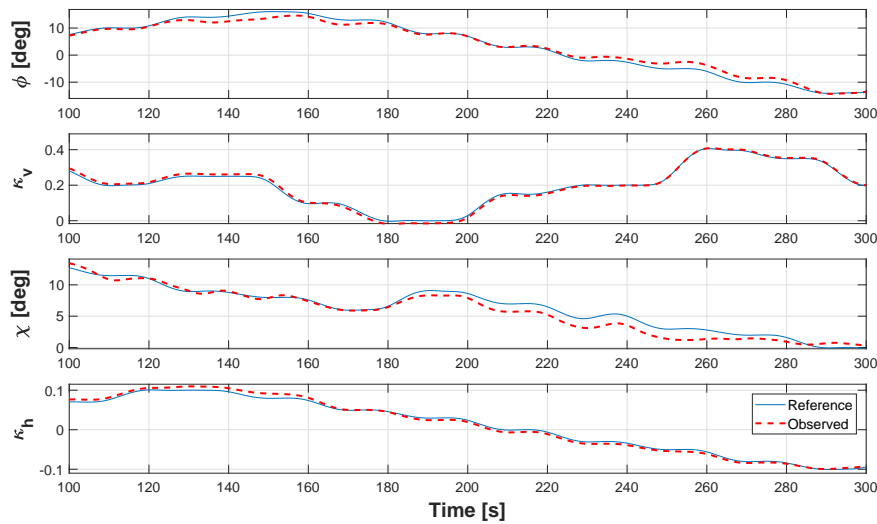


**Figure 3.** Wind state estimates in non-turbulent wind conditions with variable wind parameters at  $17 \text{ ms}^{-1}$ . Solid thick blue lines: reference wind parameters; dashed thick red lines: observations by the linear model.

### 3.3. Turbulent wind conditions

To test the estimator performance in more realistic wind conditions, several 10-minute long turbulent simulations were also considered. Starting from mean values of wind speed and inflow parameters, `TurbSim` was used to generate wind histories at 5 and 10% turbulence intensity (TI). To account for changes in the rotational speed of the machine due to turbulence, an adaptive filter was employed to extract the loads and pitch 1P harmonic components.

Figure 4 shows results at  $11 \text{ ms}^{-1}$  and 5% TI. Despite the filter-induced delay, one can notice that the estimator is capable of nicely following the fluctuations of both shears, particularly the horizontal one. On the other hand, only the mean values of the angles are well captured. A justification of this phenomenon is given in Ref. [5], where it is shown that the velocity triangle at the blade, and with it the angle of attack, is more affected by the presence of wind shear than of wind misalignment. It follows that the moments at the blades are more sensitive to shear rather than misalignment, carrying therefore more information about the first than about the latter. To better quantify the model performance, Tab. 1 and 2 show the standard deviation and the mean absolute estimation error at 5 and 10% TI. The yaw mean error for the lower turbulent case is about  $1^\circ$ , whereas for the higher turbulence level the mean error is about  $2.4^\circ$ . For yaw control, such performance should be enough, as the controller typically does not try to follow fast wind direction changes.

The model coefficients were identified starting from a set of simulations where the IPC controller was both on and off. Therefore, one should expect the linear model to be able to estimate the wind inflow both if the IPC controller is used or not. To test this hypothesis, additional 10-minute long turbulent tests were performed, using only the collective pitch controller. The standard deviation and mean absolute error with IPC off at  $11 \text{ ms}^{-1}$  with 5 and 10% TI are reported in Tab. 1 and 2. In this second scenario, the estimator seems to be slightly more accurate in computing shears and particularly angles, since now the mean error in yaw misalignment is less than  $0.5$  and  $1.3^\circ$  for low and high turbulence levels, respectively.

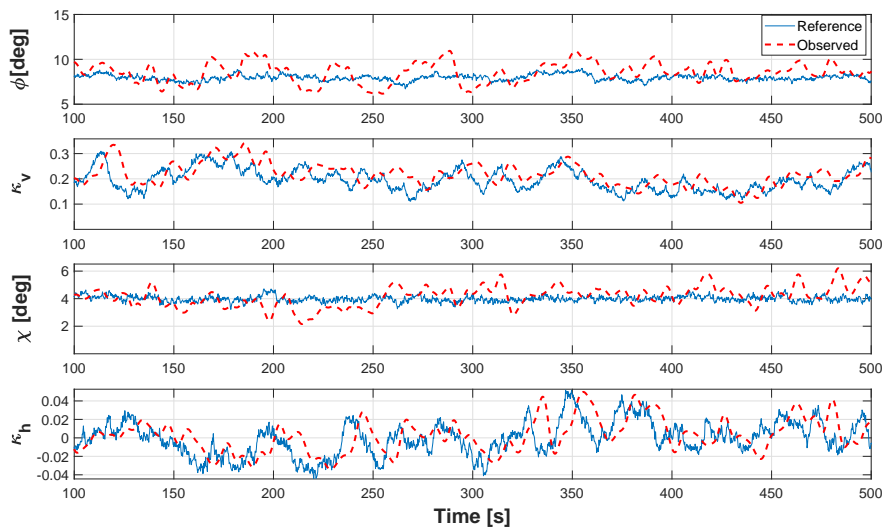


**Figure 4.** Wind state estimates in turbulent wind conditions with variable wind parameters at  $11 \text{ ms}^{-1}$ . Solid thick blue lines: reference wind parameters; dashed thick red lines: observations by the linear model.

**Table 1.** Wind state estimate standard deviation at  $11 \text{ ms}^{-1}$  and 5 and 10% TI.

Standard deviations	5% TI		10% TI	
	IPC on	IPC off	IPC on	IPC off
$\sigma_\phi$ [deg]	1.26	0.56	3.55	1.98
$\sigma_{\kappa_v}$	$3.88\text{e-}2$	$3.33\text{e-}2$	$6.77\text{e-}2$	$6.27\text{e-}2$
$\sigma_\chi$ [deg]	0.76	0.66	2.16	1.75
$\sigma_{\kappa_h}$	$1.42\text{e-}2$	$1.32\text{e-}2$	$2.92\text{e-}2$	$2.6\text{e-}2$

**Table 2.** Wind state estimate mean absolute error at  $11 \text{ ms}^{-1}$  and 5 and 10% TI.

Mean absolute error	5% TI		10% TI	
	IPC on	IPC off	IPC on	IPC off
$\epsilon_\phi$ [deg]	1.04	0.46	2.42	1.3
$\epsilon_{\kappa_v}$	$3.1\text{e-}2$	$2.58\text{e-}2$	$5.44\text{e-}2$	$4.94\text{e-}2$
$\epsilon_\chi$ [deg]	0.6	0.52	1.57	1.27
$\epsilon_{\kappa_h}$	$1.12\text{e-}2$	$1.03\text{e-}2$	$2.35\text{e-}2$	$2.04\text{e-}2$

#### 4. Conclusions

In this work, a linear formulation was proposed to relate the machine response to the wind inflow, parameterized by a vertical and horizontal misalignment angle and by a vertical and horizontal shear. Extending the idea of Ref. [5], the case of an IPC-controlled wind turbine was considered, by using the 1P harmonic of in- and out-of-plane blade bending moments and blade pitch to infer the wind conditions at the rotor disk.

The model was tested first in uniform and then in turbulent wind conditions. Based on the reported results, the following conclusions can be drawn:

- In uniform wind conditions, the model is capable of estimating the instantaneous value of both shears and angles with good precision. Small inaccuracies decrease with wind speed and are due to the linearity of the model. This can be improved with a quadratic model, as shown in Ref. [5].
- In turbulent conditions both shears can be accurately estimated, although with a delay due to the 1P extraction process. Errors of about  $1.3^\circ$  can be noted in the estimation of the yaw angle for 5% TI. Given that such errors increase with TI [5], only a mean value of such quantities can be estimated with sufficient accuracy, while instantaneous values are polluted by significant fluctuations. This problem requires further investigations to be corrected, and its origin has been explained in Ref. [5].
- The proposed formulation expands the one presented in Refs. [4, 5] to IPC-controlled turbines, but nevertheless is still capable of estimating the wind inflow even if only a collective controller is used.

### Acknowledgments

This work has been partially supported by the CL-Windcon project, which receives funding from the European Union Horizon2020 research and innovation program under grant agreement No. 727477.

### References

- [1] Bottasso CL, Croce A and Riboldi CED 2010 Spatial estimation of wind states from the aeroelastic response of a wind turbine. *The science of making torque from wind TORQUE* 2010 Heraklion, Crete, Greece.
- [2] Bottasso CL and Riboldi CED 2014 Estimation of wind misalignment and vertical shear from blade loads *Renew. Energy* **62** 293-302.
- [3] Bottasso CL and Riboldi CED 2015 Validation of a wind misalignment observer using field test data *Renew. Energy* **74** 298–306
- [4] Cacciola S, Bertelè M, Bottasso CL 2016 Simultaneous observation of wind shears and misalignments from rotor loads. *J. Phys. Conf. Ser* 2016, **753**.
- [5] Bertelè M, Bottasso CL, Cacciola S, Daher Adegas F, and Delpont S 2017 Wind inflow observation from load harmonics. *Wind Energy Sci.*, <https://doi.org/10.5194/wes-2017-23>.
- [6] Eggleston DM and Stoddard FS 1987 *Wind Turbine Engineering Design* (New York: Van Nostrand Reinhold Company Inc).
- [7] Coleman R.P. and Feingold A.M. 1958 *Theory of self-excited mechanical oscillations of helicopter rotors with hinged blades*, *Technical Report* NACA TN 1351.
- [8] Bottasso CL, Croce A, Nam Y and Riboldi CED 2012 Power curve tracking in the presence of a tip speed constraint. *Renew. Energy* **40** 112.
- [9] Riboldi CED 2012 *Advanced control laws for variable-speed wind turbines and supporting enabling technologies* Ph.D. thesis Politecnico di Milano.
- [10] Bossanyi E 2003 Individual blade pitch control for load reduction *Wind Energy*, **6** 119-8.
- [11] Bossanyi E 2005 Further load reductions with individual pitch control *Wind Energy*, **8** 481-5.
- [12] Bottasso CL and Croce A 2006-12 *Cp-Lambda: User's Manual*. *Technical Report* Dipartimento di Ingegneria Aerospaziale, Politecnico di Milano.
- [13] Jonkman BJ and Kilcher L 2012 *TurbSim User's Guide: Version 1.06.00* NREL Technical report.